Biomedical Signal Processing and Control 91 (2024) 106008

Contents lists available at ScienceDirect

Biomedical Signal Processing and Control

journal homepage: www.elsevier.com/locate/bspc

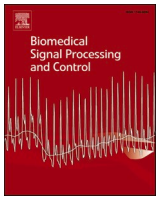

A deep 1-D CNN learning approach with data augmentation for classification of Parkinson's disease and scans without evidence of dopamine deficit (SWEDD)

Nikita Aggarwal [a,*], B.S. Saini [a], Savita Gupta [b]

[a] Department of Electronics and Communication, Dr B. R. Ambedkar National Institute of Technology, Jalandhar, India
[b] Department of Computer Science, University Institute of Technology, Chandigarh, India

ARTICLE INFO

Keywords:
Data Augmentation
Deep 1-D CNN model
Biological and Imaging-derived features
Parkinson's disease
SWEDD

ABSTRACT

Objective: Discriminating Parkinson's disease (PD) patients from the SWEDD cases remains a major challenge. Basically, SWEDD cases show normal dopamine transporter scans but are clinically suspected to mimic PD. Therefore, to avoid misdiagnosis, it is essential to know the manifestations of SWEDD in the early stages and the necessity to develop an automated diagnostic approach that can help differentiate it.
Method: In this experiment, biological and imaging-derived features are first processed using pre-processing and then, the feature engineering technique is applied to create ratio features. Afterward, a one-dimensional convolutional neural network (1-D CNN) classifier with data augmentation (DA) has been implemented for binary and multiclass classifications among three classes i.e. PD, non-PD, and SWEDD. Upton our knowledge, this proposed method has not been used before, and its results have been evaluated using various performance metrics.
Results: It is observed that the proposed method performed well using the combination of all features (biological, imaging-derived, and ratio) and achieved maximum results in terms of accuracy, f1-score, recall, and precision which are 98.71%, 98.38%, 98.71%, & 98.06% for PD vs SWEDD, 99.46%, 98.92%, 98.92% & 98.92% for PD vs non-PD, 93.84%, 94.35%, 95.38% & 93.48% for non-PD vs SWEDD, and 96.05%, 95.30%, 96.55% & 94.08% for PD vs SWEDD vs non-PD. Additionally, the results with and without the implementation of the DA technique have also been compared.
Conclusion: The proposed 1-D CNN model with the DA technique achieves the highest performance results which can help researchers find the biomarkers for disease detection.

1. Introduction

Parkinson's disease is one of the most common diseases in the family of neurodegenerative disorders [1] as it affects approximately 2 to 3 percent of the population over the age of 65 [2]. It occurs due to the significant loss of substantia nigra's dopamine neurons [3,4] and mostly, PD is typically diagnosed when 60 % to 70 % of neurons get vanished. Moreover, it has also been observed that the presence of alpha-synuclein protein in the brain may lead to the development of PD [5]. There are mainly two types of manifestations seen in PD: motor and non-motor [6]. These PD symptoms vary from person to person and the progression of the disease depends upon the individual behaviour. Sometimes, common symptoms of PD like constipation, sleep problems, slowness in walking, depression, restless legs, low blood pressure, etc. overlap with other similar disorders such as multiple system atrophy, SWEDD, essential tremor, viral parkinsonism, and others [7] which can cause the issue of misdiagnosis. Out of these similar disorders, SWEDD cases are one of the major issues that show normal dopamine transporter (DAT) imaging and are clinically suspected to mimic PD [8]. Therefore, the accurate and errorless diagnosis of PD from SWEDD or other similar disorders is a very challenging issue.

Various techniques and methodologies have been developed by our professionals or clinicians but still, there is no particular treatment found for PD cure. Therefore, early diagnosis of PD is imperative to slow down the progression of the disease. To differentiate between PD and SWEDD variants, single-photon emission computed tomography

* Corresponding author.
E-mail address: nikita.ec.19@nitj.ac.in (N. Aggarwal).

https://doi.org/10.1016/j.bspc.2024.106008
Received 28 August 2023; Received in revised form 13 December 2023; Accepted 29 January 2024
Available online 5 February 2024

(SPECT) imaging-based and cerebrospinal fluid (CSF)-based biological features have the potential to make the diagnosis at onset stages. The SPECT imaging with ^{123}I-Iofupane also called DATscan-SPECT imaging, is utilized to detect DAT functionality at the nigrostriatal dopamine neuron presynaptic nerve endings [9,10]. The amount of DAT is employed to measure the reduction of neurons in the putamen & caudate regions of the striatum with high specificity and sensitivity [11] by using striatum binding ratio (SBR), which can be a biomarker for calculating dopamine reduction [12]. So, the quantitative investigation of SBR characteristics is revealed to be a more powerful method to monitor the development of disease and treatment effects. On the other hand, CSF due to its proximity to the brain is a valuable source for the discovery of potential fluid-based optimum biomarkers for disease diagnosis. Moreover, the CSF composition may be a direct indicator of abnormal brain alterations [13] and can help in the detection of PD and SWEDD.

1.1. Reported literature

The research on early detection of PD and its similar disorders has been going on for several decades but still no clinical biomarkers or treatments have been attained. Moreover, it is also found that most research work is focused on binary classification, especially on the detection of PD from non-PD people, but PD needs to be classified from SWEDD or some other disorders. Therefore, there is a huge demand to develop an automated diagnostic method for binary and multiclass classification of disease, which may provide some level of relief to the patient or help in providing information on the progress of the disease. With advances in technology, deep learning (DL) models play a very important role in medical data analysis and can potentially diagnose PD or SWEDD patients at early stages [14]. These DL-based models analyze the data and find complicated patterns from it, which may help in the accurate diagnosis of disease.

In contrast with DL models, most of the literature is reported on traditional machine-learning (ML) algorithms in the detection of PD and SWEDD variants by using various types of datasets such as the authors of the study [15], developed the neural network (NN)-based enhanced probabilistic (EP) method for the discrimination between SWEDD and PD by using 8 clinical and imaging-derived attributes. The authors [16] extracted neural fiber connecting regions from magnetic resonance imaging (MRI) by using the tractography method. In [17], they analyzed the data based on forearm & finger movement in patients. Furthermore, [18] diagnosed the PD and SWEDD variants by using CSF characteristics. In [19], the authors applied three clustering techniques of ML on imaging-based and clinical features. Similarly, [20] used clinical features (motor and non-motor) with SBR features. The chief examination of the research was to classify SWEDD as to which category it was related to non-motor or motor manifestations of PD. Even, the study [21] utilized the resting-state tremor-based data for the detection of PD and SWEDD. Moreover, the authors [22] applied the explainable ML classifier for three binary classifications i.e. PD vs SWEDD, SWEDD vs healthy, and PD vs healthy by using clinical and SBR features.

No doubt ML classifiers are growing exponentially in the medical field but still have some limitations of ML which should be improved for better diagnosis and accurate treatment. The ML-based classifiers require handcrafted feature extraction which may lead to loss of some significant information [23]. Therefore, we developed a DL-based 1-D CNN model for the classification of PD and SWEDD to address the limitations of ML approaches. In general, CNN models have been widely explored in many medical applications such as voice recognition, neuroimaging processing, pattern recognition, and many others [24]. The main advantage of CNN models is that they can handle huge data due to multiscale architecture and can also deal with imbalanced data [25].

1.2. Literature gaps

From the above discussion, some research gaps have been found as given below:

- Given the overlap in symptoms, there is a greater likelihood of misdiagnosing PD as another ailment with comparable characteristics.
- The majority of research has focused on detecting PD in healthy cases, and there are very few studies that distinguish PD from SWEDD.
- Inadequate research has been done on the databases, due to little availability of data based on SWEDD which creates the data unbalance problem.
- Moreover, there is a lack of exploration of deep learning models due to an insufficient amount of data availability which creates the issue of over- and under-fitting of the data.
- Most of the reported research articles focus only on binary classification, but there is an exigency to develop an automated computer-based classifier for multiclass classification.

1.3. Motivation for this research work

Significant difficulties are encountered by clinicians or researchers in the diagnosis and categorization of PD from SWEDD variants due to the presence of various symptoms. The severity and complexity of the disease vary from person to person, hence the need to get diagnosed properly. To facilitate early identification, it is essential to develop reliable and accurate diagnostic and classification techniques. Many machines and deep learning models have been created to diagnose the disease in its early phases such as support vector machines (SVM) [26–29], multi-layer perceptron (MLP) [20,30–32], logistic regression (LR) [33–35], k-nearest neighbors (KNN) [34,36,37], artificial neural networks (ANN) [38–40], CNN [41–43], and many more. But still, no optimal biomarker has been found to detect the disease.

This study utilized the DL-based 1-D-CNN classifier with DA for the classification of PD and SWEDD variants. Moreover, our researchers are constantly exploring various types of data using 1-D CNN classifiers like gait patterns [44], voice signals [45], speech data [46], electroencephalography (EEG) signals [10,47], and others. In this experiment, preprocessing and feature engineering have been applied by using CSF-based biological and SPECT imaging-based SBR features. Moreover, for classification using the 1-D CNN model, huge data is required otherwise it may lead to the issue of over and under-fitting. To overcome this problem, the DA-based Gaussian distribution technique has been implemented in this experimental research work. DA is mainly used for generating synthetic data by using the available dataset and can also help in building a more stable DL-based CNN classifier [48]. Upton our knowledge, this data augmentation with 1-D CNN has not yet been implemented on these SBR and biological features in various reported literature.

1.4. Novelties and contributions

The novelties of the proposed research work are listed below:

- Many techniques and methodologies have been implemented for the discrimination of PD from non-PD (binary classification) but PD needs to be classified from SWEDD or other disorders. Therefore, the main objective of this work is to focus on multiclass classification i.e. to automatically classify the SWEDD from both PD and non-PD classes.
- To overcome the over-/under-fitting and class imbalance problems, the synthetic data has been generated by implementing the DA-based Gaussian distribution technique for this research work.

- Machine learning and deep learning algorithms are prevalent because they have achieved high classification performance. However, this research work designed the 1D CNN model with DA and applied it to imaging-derived and biological data to show its effectiveness for PD and SWEDD classification.

The chief involvement of this research study is as follows:

- For the detection of PD and SWEDD variants, the CSF-based biological and SPECT imaging-based SBR features have been utilized for this research work.
- Moreover, feature engineering has been applied to create ratio features by using biological and imaging-derived features.
- After that, the synthetic data has been generated by implementing the DA-based Gaussian distribution technique for this research work.
- After the collection of augmented data, the DL-based 1-D CNN model with the best hyper-parameters for classifying the three classes that are PD, non-PD, and SWEDD.
- The feature-wise analysis of data has been done for the three binary classification probabilities (i.e. PD vs Non-PD, PD vs SWEDD, and non-PD vs SWEDD) and one multiclass classification (PD vs Non-PD vs SWEDD).
- For a more thorough analysis, we additionally evaluate the results of the 1-D CNN classifier with and without using the DA approach.

After the brief discussion on PD and SWEDD, this article is further distributed into the following parts: (a) Section 2 describes the data & material utilized for the research work, (b) Section 3 enlightens the results found after the implementation of the 1-D CNN classifier with DA, (c) Section 4 highlights the discussion of this research study, and (d) Section 4 provides the concluding remarks of this proposed research experiment.

2. Material and techniques

In this section, the details of the dataset, the description of used features (biological and imaging-derived), data processing methods, and the implementation of various techniques for binary and multiclass classifications have been discussed. Moreover, the flow of the experimental research work is described in Fig. 1 which is presented in the following sub-sections.

2.1. Detail of database

The data was downloaded on 6th January 2023 from the PPMI database and two types of features i.e. biological features from CSF and SBR features from SPECT imaging, have been utilized for this experimental research work. In general, PPMI is a longitudinal and multinational study, the main objective of this organization is to discover optimal biomarkers for the early diagnosis of disease. A total of 675 entities (all entities belonging to the initial or screening phase) have been considered for non-PD, PD, and SWEDD people. Moreover, the demographic (age, sex) details along with sample size are provided in Table 1.

2.2. Delineation of features

2.2.1. SBR features derived from SPECT neuroimaging modality

In this experiment, a total of six SBR features are acquired from SPECT imaging using ^{123}I-Ioflupane (DaTSCAN) by using the putamen and caudate regions of the striatum. The SBR features are depicted as follows: (a) right caudate (DAT_CR), (b) left caudate (DAT_CL), (c) right putamen (DAT_PR), (d) left putamen (DAT_PL), (e) anterior of right putamen (DAT_PR_ANT), and (f) anterior of left putamen (DAT_PL_ANT). In addition, the range value of each SBR feature is provided in Table 2 for non-PD, PD, and SWEDD people. Furthermore, it is found that the feature range values of non-PD and SWEDD classes are almost near to each other, which is a very challenging task to differentiate it.

2.2.2. Biological features extracted from CSF

The biological data were acquired from the PPMI database as per the norms of the research biomarkers laboratory manual. These features are extracted from CSF and a total of four biological features have been utilized for further classification that is alpha-synuclein (α-syn), amyloid beta peptide (1–42) (Aβ $_{1\text{-}42}$), phosphorylated tau at threonine 181

Table 1
The demographic detail along with sample size for Non-PD, PD & SWEDD people.

Variable	Non-PD	PD	SWEDD
Sample size	160	460	55
Age[#]	60.89 ± 11.23	61.55 ± 9.91	60.4 ± 10.55
Sex (Female/Male)	53/107	178/282	23/32

[#] Age is measured as (Mean ± SD).

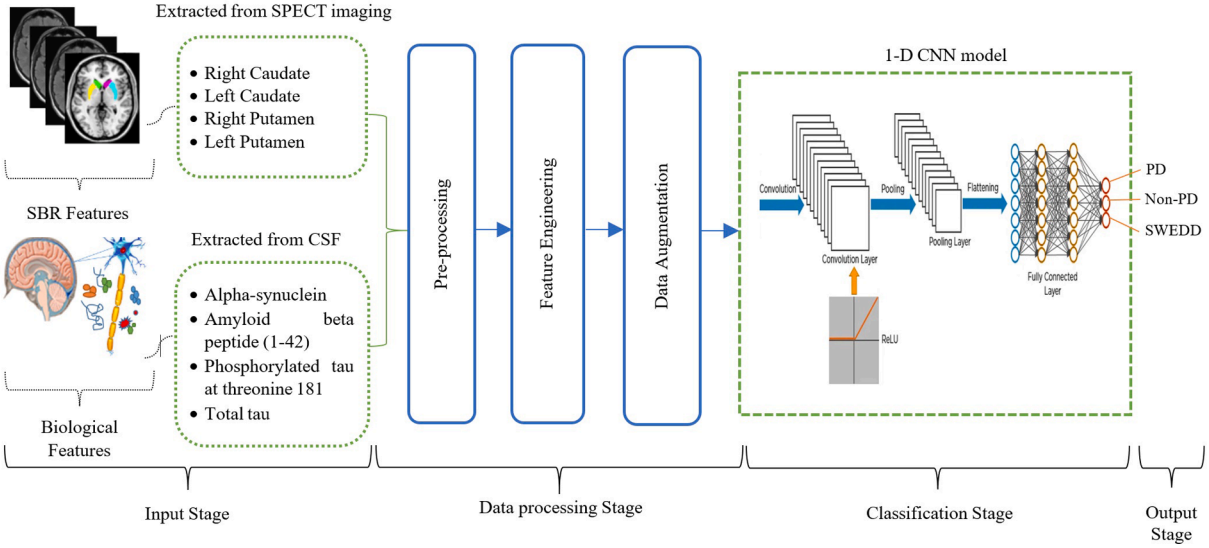

Fig. 1. The flow diagram of the proposed research work.

Table 2
The range of each SBR feature (Mean ± SD) for Non-PD, PD & SWEDD people.

Variable	Non-PD	PD	SWEDD
DAT_CR	2.99 ± 0.64	1.97 ± 0.60	2.83 ± 0.62
DAT_CL	3.04 ± 0.67	1.97 ± 0.59	2.87 ± 0.59
DAT_PR	2.14 ± 0.61	0.82 ± 0.36	2.09 ± 0.53
DAT_PL	2.14 ± 0.59	0.80 ± 0.35	2.05 ± 0.52
DAT_PR_ANT	2.63 ± 0.62	1.32 ± 0.47	2.52 ± 0.54
DAT_PL_ANT	2.61 ± 0.60	1.28 ± 0.46	2.49 ± 0.57

($ptau_{181}$), and total tau (tTau). The range value of each biological feature is provided in Table 3 for non-PD, PD, and SWEDD people. From Table 3, it is also observed that the features α-syn and $A\beta_{1\text{-}42}$ have much larger values compared to other biological features ($ptau_{181}$ and tTau).

2.3. Graphical representation of features

For more understanding of the relationship between various features for three classes i.e. non-PD, PD, and SWEDD, the graphical representation has been shown by using the violin-strip plots (in Fig. 2). The merging of two plots in one plot gives a better interpretation of data, where violin plots provide information on the probability density of data (which can be observed by the shape of the curve), and strip plots are used to visualize the distribution of many individual one-dimensional values. From the graphs, it has been observed that there is an overlapping of the data points in the same range among the three classes that are too difficult to distinguish the class category. Moreover, it also found that in comparison to SBR features, biological features have a higher value range.

2.4. Pre-processing and feature engineering

The issues with large and small range values of features can be overcome by applying the scaling technique of pre-processing to each feature. And, when all features are on the same scale, it can also help the algorithm better understand the relative relationship. Therefore, for this experiment, the min–max normalization is used as a pre-processing technique for scaling the data that helps in increasing the accuracy as well as reliability. This normalization performs a linear transformation on the data and also scales all the values in the range of 0 to 1. The pseudocode of the pre-processing technique is provided in algorithm 1. The formula representation of min–max normalization is given as $X'_{i(scaled)} = \frac{X - X_{min}}{X_{max} - X_{min}}$.

Algorithm 1 ***Pseudocode of Pre-processing.***

Input: *Data set* $(D_i) = \{F_1, F_2, \ldots, F_n\}$ *// Imaging-derived and biological features* $(n = 10)$.
Output: $X^i_{j(Norm)}$ *// Normalized values of each features*
Identify Maximum and Minimum values of each feature (X_{max}, X_{min})
for $i = 1$ *to* 10 *do // i are the selected features*
for $j = 1$ *to* 675 *do // each feature consists of j elements*

$$X^i_{j(Norm)} = \left(\frac{X_j - X_{min}}{X_{max} - X_{min}}\right); \text{// Update the normalized value for each feature}$$

end for j
end for i

After pre-processing, the feature engineering technique is also used to create new features from the existing features [49] by adjusting or transforming features. The ratio features have been created by selecting two existing features at a time and after that identifying the higher-value and lower-valued features. A total of six ratio features has been utilized that are ptau $_{181}$/tTau, tTau/Aβ $_{1\text{-}42}$, ptau/Aβ $_{1\text{-}42}$, DAT_CR/DAT_CL, DAT_PR/DAT_PL, and DAT_PR_ANT/DAT_PL_ANT. These ratio features might have the capability to detect PD and SWEDD in the early stage [50]. Moreover, the study [51] showed that the CSF levels of the ratios p-tau/tau and p-tau/b-amyloid at baseline can indicate the development of motor symptoms in PD. For this research, these ratio features are used along with the original SBR and biological features. In addition, the detail of each ratio feature is given in Table 4 for non-PD, PD & SWEDD people. Also, the pseudocode of feature engineering is given in algorithm 2.

Table 3
The range of each Biological feature (Mean ± SD) for Non-PD, PD & SWEDD people.

Variable	Non-PD	PD	SWEDD
Aβ $_{1\text{-}42}$	1036.46 ± 514.55	915.76 ± 406.63	969.14 ± 352.25
α-syn	1710.70 ± 514.54	1532.28 ± 406.62	1683.94 ± 352.25
ptau $_{181}$	17.19 ± 8.88	14.40 ± 5.67	15.49 ± 6.05
tTau	19.14 ± 83.79	169.94 ± 61.66	178.53 ± 61.23

Algorithm 2 ***Pseudocode of Feature Engineering.***

Input: $X^i_{j(Norm)}$ *// Normalized values of existing features*
Output: *Set of existing* (F_i) *and created new features* (F_k)
for $k = 1$ *to* 6 *do*
for i do
for j do
Select two features at a time, each containing j elements.
Identify highest valued and lower valued feature from selected features.

$$F^k_{j(new)} = \left(\frac{Lowervaluedfeature}{Highervaluedfeature}\right); \text{// create new features.}$$

end for j
end for i
end for k

2.5. Data augmentation

Lack of labeled data for model training and over-/under-fitting of the data are two major issues in the training of supervised models [52]. Therefore, the DA technique can be used to overcome these issues [48]. Basically, DA refers to a collection of methods that improve the quantity and quality of training datasets by creating synthetic datasets and also have the potential to enable the development of more accurate DL classifiers using such datasets [53]. In this experiment, the data is transformed by adding a random noise sample to the data. The Gaussian distribution p (x; μ, σ) has been utilized to generate the synthetic data, where the variable p (random variable (x); mean (μ), standard deviation (σ)) is defined by its probability density function (PDF) and equal to (1 / (σ√(2π))) * eˆ(-(x-μ) ^{2} / (2σ^2)). Furthermore, the DA technique is applied only on the minority class to balance the data with the majority class for each classification. The pseudocode for data augmentation is provided in algorithm 3.

Algorithm 3 ***Pseudocode of Data Augmentation***

2.6. Classifier (1-D CNN)

The 1-D CNN classifier has been utilized for the discrimination between the three classes which are PD, non-PD, and SWEDD variants. Basically, it is a sort of deep neural network and is mainly utilized for one-dimensional data like time series data, text, etc. In this experiment, the biological, SBR, and ratio features have been utilized. As can be seen in Fig. 3, the 1-D CNN model comprises the following layers: input, three 1-D convolutional layers, pooling, dropout, fully connected (flatten), two dense, and output.1.

The convolutional layer involves the convolutional operation and also it is the backbone of the CNN architecture. The calculation of the convolutional layer is given as input data x ∈ ℝˆn and a set of filters w ∈ ℝˆm, the output feature map y is obtained by performing a convolution operation. The convolution procedure can be defined as y[a] = f (w * x [a: a + m-1] + b), where x [a: a + m-1] represents a subsequence of x of length m starting from index a. The filter w is applied to this subsequence, and the dot product between w and the subsequence is calculated. The bias term b is added to the result, and the activation function f (·) is implemented element-wise to introduce non-linearity. In this

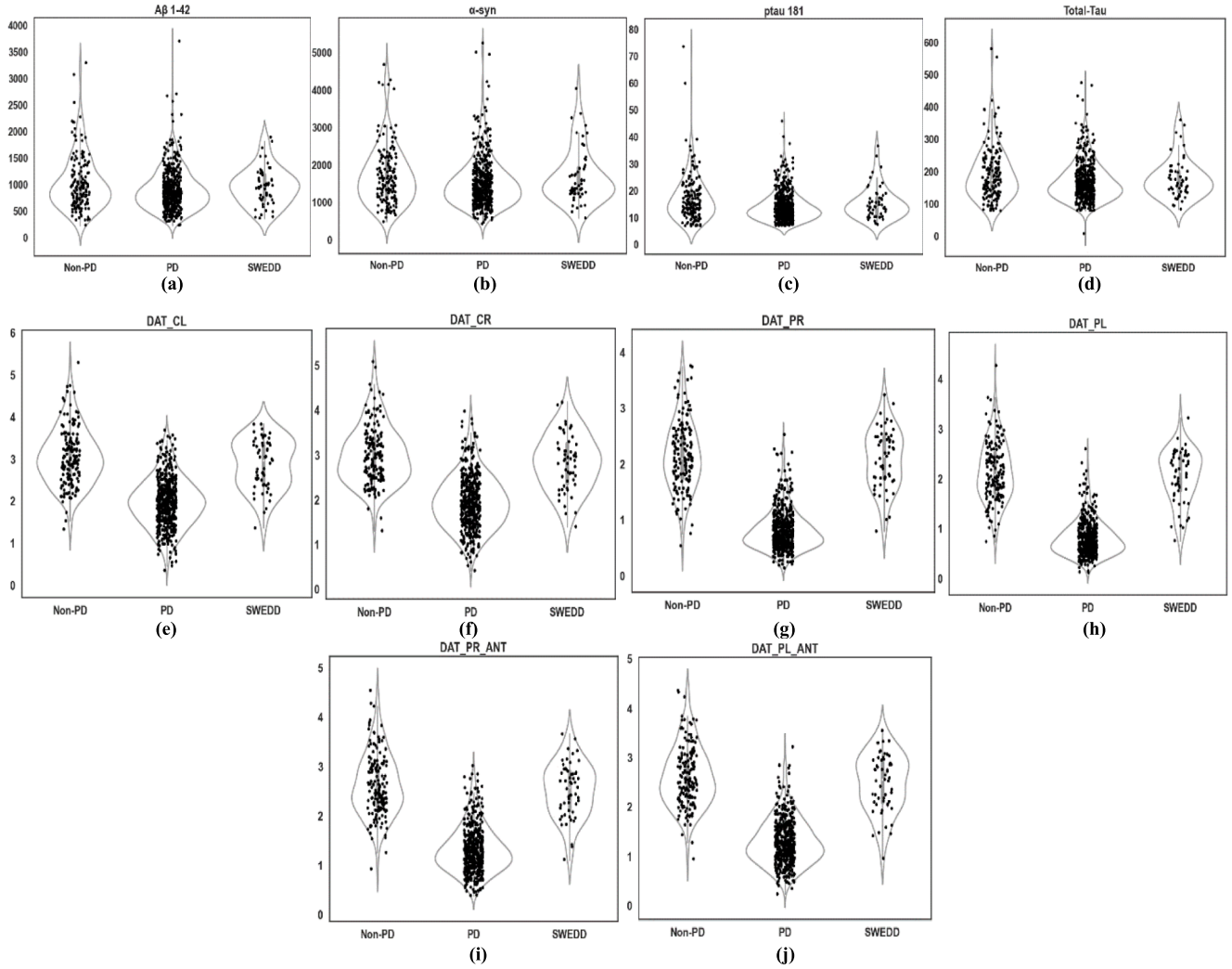

Fig. 2. The violin-strip plots ((a)-(j)) representation of various biological and SBR features for non-PD, PD, and SWEDD variants.

Table 4
The range of each ratio feature (Mean ± SD) for Non-PD, PD & SWEDD variants.

Category	Variable	Healthy	PD	SWEDD
Biological-based ratio features ($R_{Biological}$)	ptau $_{181}$/tTau	0.09 ± 0.01	0.08 ± 0.04	0.09 ± 0.01
	tTau/Aβ $_{1\text{-}42}$	0.22 ± 0.16	0.20 ± 0.09	0.19 ± 0.08
	ptau/Aβ $_{1\text{-}42}$	0.019 ± 0.018	0.017 ± 0.009	0.017 ± 0.008
SBR-based ratio features (R_{SBR})	DAT_CR/DAT_CL	0.98 ± 0.09	1.01 ± 0.24	0.98 ± 0.09
	DAT_PR/DAT_PL	1.01 ± 0.14	1.14 ± 0.56	1.03 ± 0.18
	DAT_PR_ANT/ DAT_PL_ANT	1.01 ± 0.09	1.08 ± 0.35	1.02 ± 0.13

research work, a total of three convolutional layers have been involved that are C_1, C_2, and C_3 with different filter sizes of 32, 64, and 128 respectively. Each layer used leaky ReLU (rectified linear unit) as an activation function with a kernel size of (3,1) and in addition, this leaky ReLU function is notated as f(x) = max (0.01 * x, x). These activation functions are applied element-wise to the outputs of the convolutional layer or fully connected layers.

After that, the results from convolutional layers, the max pooling layer has been used with a pool size of (3,1) and stride rate of 2. This layer calculates the maximum value from the patched feature map to create a down-sampling. The dropout layer randomly "drops out" or deactivates a fraction of neurons during training. This reduces overfitting, which happens when a network memorizes training material and cannot generalize. The network learns more robust, non-training data-specific properties by randomly deleting neurons [47]. Hereafter, a fully connected layer performs high-level feature extraction and makes predictions based on the learned features. The outputs from the previous layer, whether it's a convolutional layer or a pooling layer, are flattened into a 1D vector. In a fully connected layer, all of the neurons from the preceding layer are linked to each of the neurons in the current layer through weights and biases. The output of a fully connected layer may be calculated as follows: y = f (Wx + b). Lastly, the two dense layers have been utilized i.e. D_1 and D_2 with filter sizes of 256 & 512 respectively. The last layer of the 1D CNN is the output layer. Moreover, a softmax activation function is generally used for the classification to obtain probability distributions over multiple classes. The softmax function takes the outputs of the previous layer and normalizes them to represent probabilities. The mathematical expression of the softmax function is $S(y_a) = \exp(y_a)/\sum_{j=1}^{n}\exp(y_a)$.

Finally, the cross-entropy (CE) loss function for classification has been used to distinguish among three classes i.e. non-PD, PD, and SWEDD variants. It measures the difference between the expected and the actual output. The model is perfect when the loss function is 0. $CE = \sum_{a=1}^{n} x_a \exp S(y_a)$, where x_a is the actual value and $S(y_a)$ is the softmax probability for ath class. Moreover, the Adam optimizer is utilized to

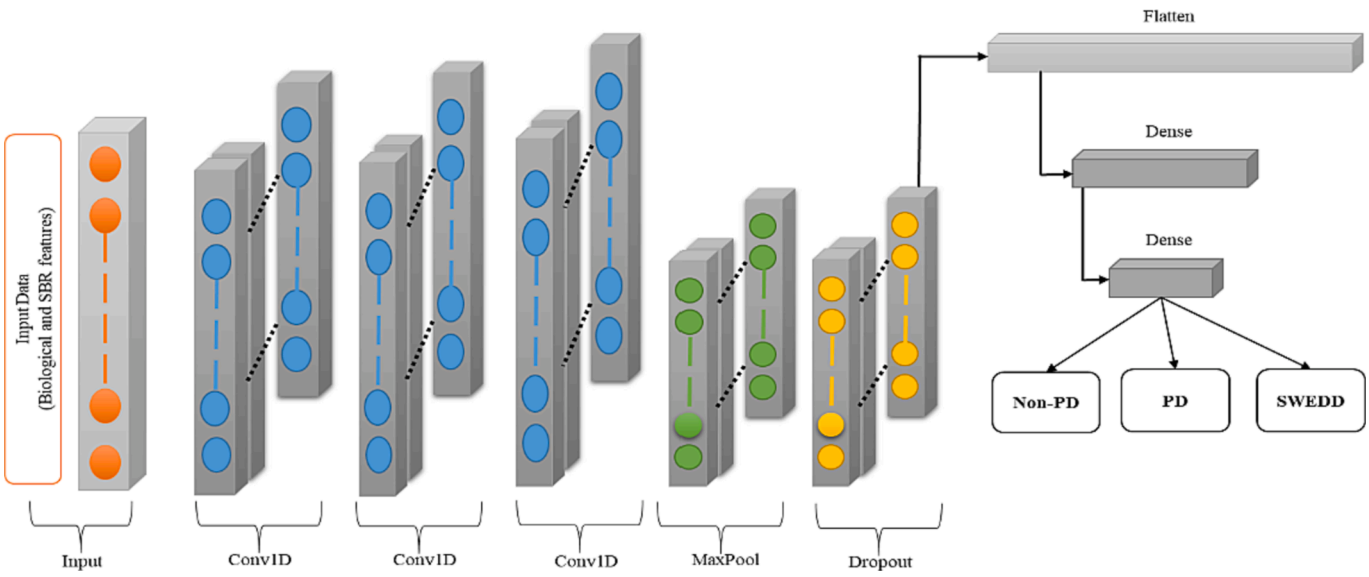

Fig. 3. Block diagram of 1-D CNN model.

reduce the categorical cross-entropy loss and the hyper-parameters were used as follows: $\alpha = 0.001$, $\beta 1 = 0.9$, $\beta 2 = 0.999$, $\epsilon = 10^{-8}$.

3. Experimental results

The 1-D CNN model has been analyzed by using various performance metrics because calculating the accuracy parameter only for any model is not sufficient to declare whether the model is performing well or not [54]. Therefore, for more analysis of the performance of the model in detail, some other parameters have been discussed such as recall (or sensitivity), precision, and F1-score in addition to accuracy metric parameters for both binary and multiclass classifications in this research work. These performance metrics are defined as follows: (a) Recall = $TR_{(+)} / TR_{(+)} + FA_{(-)}$, (b) Precision = $TR_{(+)} / TR_{(+)} + FA_{(+)}$, (c) F1-score = $2^* TR_{(+)} / 2^* TR_{(+)} + FA_{(+)} + FA_{(-)}$, and (d) Accuracy = $TR_{(+)} + TR_{(-)} / TR_{(-)} + TR_{(+)} + FA_{(+)} + FA_{(-)}$, where $TR_{(-)}$, $TR_{(+)}$, $FA_{(+)}$, and $FA_{(-)}$ are the true positive, true negative, false positive, and false negative respectively.

All research experiments have been done after augmentation of data, to remove the issue of imbalance of data. The original data is split into the ratio of 30 %:70 % as testing: training data. After that, the augmentation is implemented on only 70 % of the training data and generates the synthetic data. These experiments are executed on the 64-bit operating system of Intel (R) W-2255 CPR @ 3.70 Giga-hertz with RAM of 128 GB. Furthermore, with the aim of providing a more accurate evaluation, feature-wise analysis of all binary and multiclass classifications has been performed.

In Table 5, the outcomes of the comparison between various features for classifying PD and non-PD people are discussed. In this binary classification, the DA technique has only been applied to non-PD people (i.e. two times from the original training sample size), to equalize the sample size with non-PD people. From the outcomes, it has been observed that the individual use of SBR or biological features does not perform well as compared to the combinational set of these features. No doubt, the combination of SBR and biological features has shown favorable outcomes across performance metrics but still falls low. Therefore, these results have been enhanced by combining certain ratio features with SBR and biological features. As a consequence, the accuracy, f1 score, recall, and precision of these results have been reached to be 99.46 %, 98.92 %, and 98.92 %, respectively.

Besides, Table 6 shows that the 1-D CNN classifier also performed well in differentiating SWEDD and PD using a combinational set of SBR and biological with ratio features. In this case, the DA technique has only been applied on SWEDD variants i.e. nine times from the original training sample size, so as to equalize the sample size with PD. The outcomes yielded for various performance metrics in terms of accuracy, F1-score, recall, and precision are 98.71 %, 98.38 %, 98.71 %, and 98.06 % respectively. As compared to others, the lowest results have been shown by biological features i.e. 93.54 %, 95.47 %, 94.83 %, & 96.12 % in accuracy, F1-score, recall, and precision respectively.

After that, the results obtained for the classification of non-PD and SWEDD are lower than those of other binary classifications. Without a doubt, it is quite difficult to differentiate between people with SWEDD and those who do not have PD since the values of these two groups are practically the same, as shown in Fig. 2. Therefore, the proposed method has the potential to discriminate up to some level. This 1-D CNN model with the DA technique has been applied to distinguish non-PD people and SWEDD cases using a combination set of SBR and biological features along with ratio features and it was found that the results varied significantly as seen in Table 7. The obtained results are 93.84 %, 94.35 %, 95.38 %, and 93.84 % in terms of accuracy, F1-score, recall, and precision respectively.

Based on the findings of binary probabilities shown above, it is also pointed out that most of the published research relies on binary

Table 5
Comparison between various features for PD and non-PD binary classification.

S. No.	Features	Accuracy	F1-Score	Recall	Precision
1	SBR	97.84 %	94.86 %	93.54 %	96.23 %
2	Biological	94.09 %	96.49 %	96.23 %	96.77 %
3	SBR + Biological	97.84 %	97.54 %	97.84 %	97.31 %
4	**SBR + Biological + R_{SBR} + $R_{Biological}$**	**99.46 %**	**98.92 %**	**98.92 %**	**98.92 %**

Table 6
Comparison between various features for PD and SWEDD binary classification.

S. No.	Features	Accuracy	F1-Score	Recall	Precision
1	SBR	95.48 %	94.12 %	93.54 %	94.83 %
2	Biological	93.54 %	95.47 %	94.83 %	96.12 %
3	SBR + Biological	98.06 %	97.74 %	98.06 %	97.42 %
4	**SBR + Biological + R_{SBR} + $R_{Biological}$**	**98.71 %**	**98.38 %**	**98.71 %**	**98.06 %**

Table 7
Comparison between various features for non-PD and SWEDD binary classification.

S. No.	Features	Accuracy	F1-Score	Recall	Precision
1	SBR	87.69 %	89.98 %	89.23 %	90.76 %
2	Biological	81.53 %	80.76 %	80 %	81.54 %
3	SBR + Biological	81.53 %	83.04 %	86.15 %	83.04 %
4	**SBR + Biological + R_{SBR} + $R_{Biological}$**	**93.84 %**	**94.35 %**	**95.38 %**	**93.84 %**

classification; However, the SWEDD class would have to be distinct from both the PD class and the non-PD class to be considered distinct. Therefore, in this research work, a 1-D CNN model is also implemented for multiclass classification to discriminate all three classes as shown in Table 8. From the results, it is observed that this deep 1-D CNN classifier has the potential to distinguish and has given very good results i.e. 96.05 %, 95.30 %, 96.55 %, and 94.08 % accuracy, F1-score, recall, and precision. The lowest results are provided by the classifier if only biological features have been utilized for classification.

Moreover, the feature-wise analysis has been done among all binary and multiclass classifications for the evaluation of various performance metrics by presenting graphical representation (histograms) as illustrated in Fig. 4. From all the histogram graphs, it has been seen that the combination of all the features (biological + SBR + ratio) performed well among others. The lowest results are provided by the classifier if only either biological or SBR features have been utilized for classification.

4. Discussion

Medically, SWEDD is a heterogeneous syndrome and radiological diagnosis [17]. The clinical diagnosis of SWEDD variants from both PD and non-PD (healthy people) at an early stage is very problematic. Mainly, research on the early detection of PD and its similar disorders has been going on for several decades but still, no clinical biomarkers or treatments have been attained. Moreover, it is also found that the published work is mostly focused on binary classification, especially on the detection of PD from non-PD people, but PD needs to be classified from SWEDD or other disorders. Therefore, there is a huge demand to develop an automated diagnostic method for binary or multiclass classification of disease, which may provide some level of relief to the patient or help in providing information on the progress of the disease.

In this experimental research work, SPECT imaging-based SBR and biological features have been utilized to differentiate between PD and SWEDD variants. These SBR and CSF-based biological features have the potential to make the diagnosis at early stages. In general, the loss of neurons in the putamen & caudate regions of the striatum can be measured by using SBR values [12] with high specificity and sensitivity [11]. Normally, many studies have utilized only the four types of SBR features i.e. DAT_CR, DAT_CL, DAT_PR, and DAT_PL. But, in this study, the authors used two more SBR features that belong to the anterior part of the putamen that are DAT_PR_ANT and DAT_PL_ANT, which may play a significant role in detecting the disease. Moreover, the CSF composition may be a direct indicator of abnormal brain alterations [13] and can help in the detection of PD and SWEDD. Also, the ratio features have been created by implementing feature engineering techniques from existing SBR and biological features. Mainly, this feature engineering provides robust results in the diagnosis of disease and also reduces the complexity of the models [54].

Table 8
Comparison between various features for PD and SWEDD and non-PD multiclass classification.

S. No.	Features	Accuracy	F1-Score	Recall	Precision
1	SBR	91.13 %	91.36 %	90.64 %	92.11 %
2	Biological	90.14 %	89.12 %	88.17 %	90.09 %
3	SBR + Biological	92.11 %	91.85 %	93.10 %	90.64 %
4	**SBR + Biological + R_{SBR} + $R_{Biological}$**	**96.05 %**	**95.30 %**	**96.55 %**	**94.08 %**

With advances in technology, DL and ML models play a very vital role in medical lines and also have the ability to diagnose PD or SWEDD patients at an earlier stage [14]. Some reported studies that have discriminated between PD and SWEDD by using various ML and DL classifiers such as the authors of the study [15], developed the EPNN method by using 8 clinical features and achieved an accuracy of 95.3 % for the classification between SWEDD and PD. The authors [16] extracted neural fiber connecting regions from MRI by using the tractography method and got 77.92 % accuracy. Furthermore, [18] discriminates the PD and SWEDD variants by using CSF and clinical characteristics and the authors obtained a p-value less than 0.001. In [19], the authors applied three clustering techniques of ML on imaging-based and clinical features. The authors achieved the maximum results from the hierarchical clustering technique in terms of accuracy, sensitivity, specificity, and f1-score of 64 %, 78.13 %, 38.89 %, and 73.53 % respectively. Even, the study [21] utilized the resting-state tremor-based data for the detection of PD and SWEDD and found that PD patients indicated greater angular velocity signals than the SWEDD variant at $p < 0.05$ significance level. Moreover, [55] implemented CNN classifier by using SPECT imaging data whereas the study [56], also used SPECT imaging to classify SWEDD and PD by implementing the 3D CNN approach and got approximately 82 % accuracy.

Furthermore, these ML classifiers are growing exponentially in the medical field but still have some limitations of ML which should be improved for better diagnosis and accurate treatment. The ML-based classifiers require handcrafted feature extraction which may lead to loss of some essential information. Therefore, to avoid the problems of ML methods, DL-based models can be used for the detection of disease at its early stages. Basically, these DL-based models can analyze the data and find complicated patterns from it, which may help in the accurate diagnosis of disease. Moreover, the DL-base 1-D CNN model has been utilized on SBR and biological features with built-in ratio features for the classification of PD and SWEDD in this experimental research work. The selected hyper-parameters of the 1-D CNN classifier are best suited for disease detection and this is concluded after several examinations of different combinations of parameters. For classification, huge data is required by DL models otherwise it may lead to the issue of over and under-fitting. To overcome this problem, the DA-based Gaussian distribution technique has been implemented to create the synthetic data and can also help in reducing the class unbalance problem. In general, this DA can only be applied to training data, and for this experiment, the training data was taken from 70 % of the original data, and 30 % data was fixed for testing.

After the collection of augmented data, the feature-wise analysis of data has been done by using a 1-D CNN model for the three binary classification probabilities (i.e. PD vs non-PD, non-PD vs SWEDD, and PD vs SWEDD) and one multiclass classification (PD vs non-PD vs SWEDD). From the outcomes, it has been noticed that the 1-D CNN model performed well among all classifications. Even the outcomes of the classifier are also compared with and without the implementation of the DA, technique are discussed in Table 9, which can help the researchers in their future work for better evaluation and disease detection.

In addition, the radar graphs are also depicted in Fig. 5 for better interpretation as sometimes different quantitative scales need to be visualized simultaneously. From the graphs, it has been observed that by using the data augmentation technique the results have been improved and it can be seen for all classification probabilities. A huge change is noticed for PD vs SWEDD and PD vs SWEDD vs non-PD classifications

Fig. 4. Histogram graphs ((a)-(d)) of feature-wise analysis among all binary and multiclass classifications for the evaluation of various performance metrics.

Table 9
Comparison between the results with and without using data augmentation.

Category	Without Augmentation				With Augmentation			
	Accuracy	F1-Score	Recall	Precision	Accuracy	F1-Score	Recall	Precision
PD vs SWEDD	90.32 %	89.91 %	89.74 %	90.09 %	98.71 %	98.38 %	98.71 %	98.06 %
PD vs Non-PD	93.01 %	91.18 %	91.93 %	90.32 %	99.46 %	98.92 %	98.92 %	98.92 %
Non-PD vs SWEDD	64.61 %	59.83 %	56.92 %	63.07 %	93.84 %	94.35 %	95.38 %	93.84 %
PD vs Non-PD vs SWEDD	83.74 %	82.99 %	83.74 %	82.26 %	96.05 %	95.30 %	96.55 %	94.08 %

than other classifications.

Moreover, there are many studies in which CNN models with DA techniques have been broadly used for PD detection by applying different datasets such as [48], the authors used the generative adversarial networks (GAN) as a DA technique to enhance the data's sample size and also applied the CNN-based Alex net model for classification. The study [57] utilized the Xception model with six DA techniques by implementing voice data. The authors [58] applied the CNN model to wearable sensor data and got a huge change in results after the DA technique was approved from 77.54 % to 86.88 %. of accuracy. In [59], GAN was used to synthesize digital drawing tests acquired from PD and non-PD people. The four architectures of drawings were StyleGAN2-ADA, StyleGAN3, StyleGAN2-ADA + LeCam, and projected GAN. The study [60], used figure drawings for detecting PD patients from healthy people by applying the CNN model with DA. Besides, [61] implemented the gait data for the discrimination between PD and non-PD people. Therefore, the comparison results in terms of accuracy, sensitivity, and specificity between these studies have been discussed in Table 10.

4.1. *Significance of the proposed study*

Discriminating PD patients from the SWEDD cases remains a major challenge. In general, SWEDD variants show normal dopamine transporter scans but are suspected to mimic PD clinically. Therefore, to avoid misdiagnosis, the early detection of PD and SWEDD is imperative and needs to differentiate the symptoms of them. Although many strategies and methods have been developed by our professionals or physicians but still, no specific treatment has been found to cure the disease. Hence, DL models have the capability to detect subtle patterns and changes in medical data that may occur before noticeable symptoms. Moreover, these DL-based models can allow healthcare professionals or doctors to initiate appropriate treatment plans and strategies to slow the progression of the disease. Therefore, in this experiment, a deep learning-based 1-D CNN model with the DA technique has been proposed using SBR and biological features with created ratio features. From the results, it has been observed that the proposed method may lead to earlier initiation of treatment and support, potentially improving patient outcomes and quality of life. Moreover, many studies have utilized only the four types of SBR features i.e. right caudate, left caudate, left putamen, and right putamen. But, in this study, the authors used two more SBR features that belong to the anterior parts (left and right) of the putamen, which may play a significant role in detecting the disease. The main focus of this study is on multiclass classification i.e. to automatically classify the SWEDD from both PD and non-PD classes which is a very challenging part. By providing additional insights and analysis, these models assist clinicians in making informed decisions about patient care, especially in complex cases. Furthermore, this proposed method contributes to a deeper understanding of the disease and may lead to the development of novel therapeutic targets.

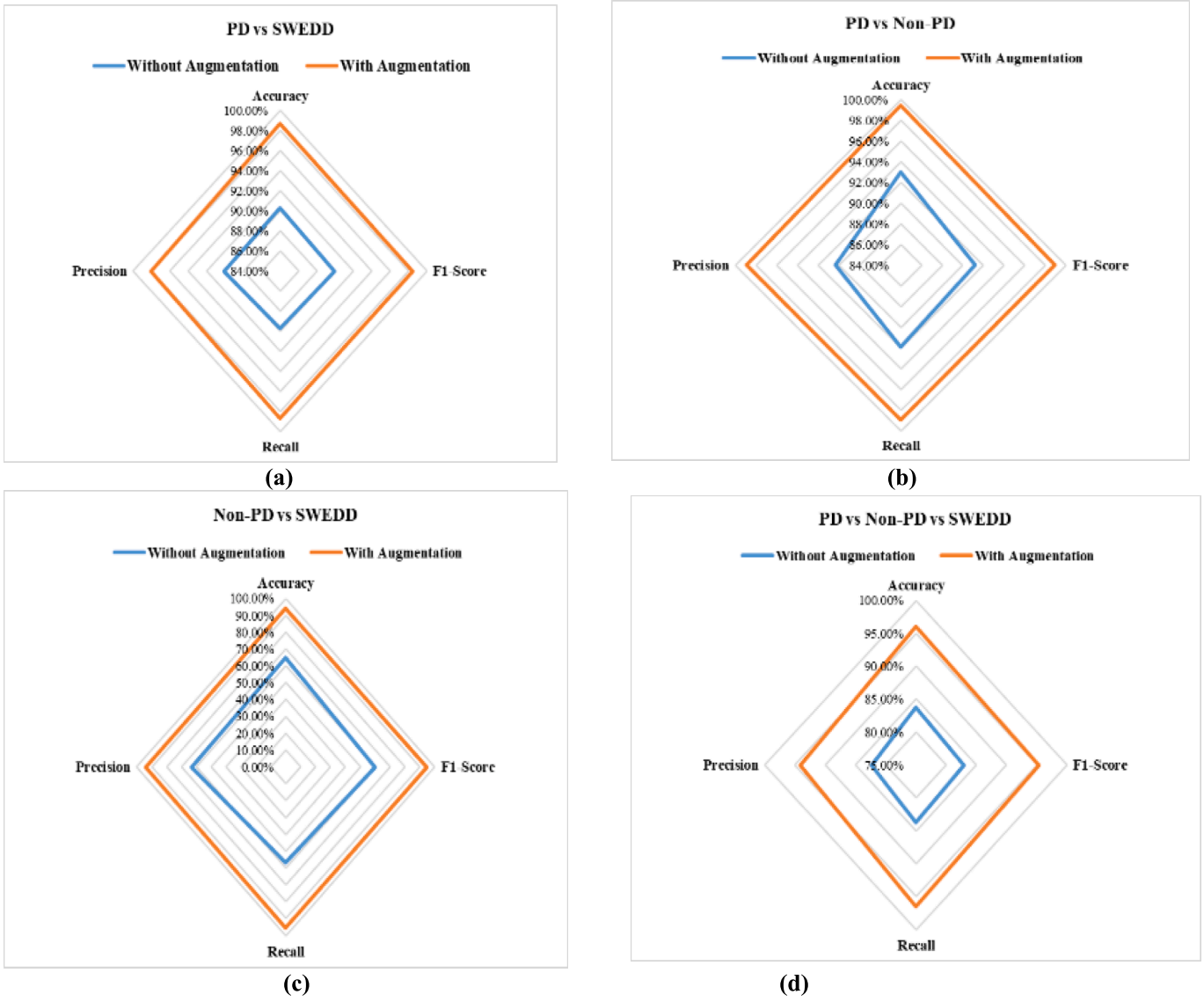

Fig. 5. Radar graph for comparison visualization with and without the implementation of DA technique for various binary and multiclass classifications.

Table 10
Comparison between various reported studies.

Reference	Subjects	Implemented Data	Classification	Performance		
				Accuracy	**Sensitivity**	**Specificity**
[48]	PD 67 Non-PD 85	MRI images	PD vs non-PD	89.23 %	–	–
[57]	PD 50 Non-PD 50	Voice data	PD vs non-PD	82.12 %	–	–
[59]	PD 422 Non-PD 146	Digital and hand-drawn Archimedean spiral drawings	PD vs non-PD	–	96.6 %	69.7 %
[60]	PD 58 Non-PD 29	Figure-drawings time series	PD vs non-PD	95.02 %	–	98.31 %
[61]	PD 58 Non-PD 29	Gait	PD vs non-PD	95.51 %	96.59 %	94.44 %
Proposed	**PD 460** **Non-PD 160** **SWEDD 55**	**SBR and biological features**	**PD vs SWEDD** **PD vs Non-PD** **Non-PD vs SWEDD** **PD vs Non-PD vs SWEDD**	**98.71 %** **99.46 %** **93.84 %** **96.05 %**	**98.71 %** **98.92 %** **95.38 %** **96.55 %**	– – – –

5. Conclusion

Due to similar symptoms of PD and other disorders, the potential for overlapping and misdiagnosis is high. The research on the detection of PD from SWEDD or other similar disorders has been going on for several decades but still no clinical biomarkers or treatments have been attained. Moreover, it has been shown that most research work is concentrated on binary classification, especially on the detection of PD

from non-PD people, but diagnosis of PD needs to be classified from SWEDD or other disorders. Therefore, there is a significant demand for the development of an automated diagnostic method for binary and multiclass classification of disease, which may provide some level of relief to the patient or help in providing information on the progress of the disease. In this experiment, the 1-D CNN model with the DA technique has been applied to show its effectiveness for the three binary classification probabilities and one multiclass classification. From the outcomes, it has been observed that the proposed method achieves the highest performance results among all classification probabilities by using SBR and biological features with ratio features. Besides the advantages, some shortcomings need to be addressed in future work. Firstly, the small number of SWEDD participants in the dataset used in this study may reduce the generalizability of the proposed model and secondly, a limited amount of features have been employed in the 1-D CNN model for computation that can be cost-effective. Hence, the benefits and shortcomings of this proposed study may assist medical professionals or experts in identifying biomarkers to differentiate PD and SWEDD.

CRediT authorship contribution statement

Nikita Aggarwal: Conceptualization, Methodology, Visualization, Writing – original draft. **B.S. Saini:** Supervision, Writing – review & editing. **Savita Gupta:** Conceptualization, Supervision, Visualization.

Declaration of competing interest

The authors declare that they have no known competing financial interests or personal relationships that could have appeared to influence the work reported in this paper.

Data availability

The authors do not have permission to share data.

Acknowledgments

PPMI is a public-private partnership supported by the Michael J. Fox Foundation for Parkinson's Research and several pharmaceutical and biotechnology companies. These companies include Abbott Laboratories, GE Healthcare, Avid Radiopharmaceuticals, Bristol-Myers Squibb, Covance, Élan, Genentech, GlaxoSmithKline, Eli Lilly and Company, Merck & Co., Meso Scale Discovery, Pfizer, Hoffmann-La Roche, UCB

References

[1] E. Kaplan, et al., Novel nested patch-based feature extraction model for automated Parkinson's Disease symptom classification using MRI images, Comput. Methods Programs Biomed. 224 (2022) 107030, https://doi.org/10.1016/j.cmpb.2022.107030.

[2] M. Tanveer, A.H. Rashid, R. Kumar, R. Balasubramanian, Parkinson's disease diagnosis using neural networks: survey and comprehensive evaluation, Inf. Process. Manag. 59 (3) (2022) 102909, https://doi.org/10.1016/j.ipm.2022.102909.

[3] N. Aggarwal, B.S. Saini, S. Gupta, "The impact of clinical scales in Parkinson's disease: a systematic review", Egypt. J. Neurol. Psychiatry Neurosurg. 57 (1) (2021) https://doi.org/10.1186/s41983-021-00427-9.

[4] T. Tuncer, S. Dogan, U.R. Acharya, Automated detection of Parkinson's disease using minimum average maximum tree and singular value decomposition method with vowels, Biocybern. Biomed. Eng. 40 (1) (2020) 211–220, https://doi.org/10.1016/j.bbe.2019.05.006.

[5] R. Prashanth, S. Dutta Roy, P.K. Mandal, S. Ghosh, Automatic classification and prediction models for early Parkinson's disease diagnosis from SPECT imaging, Expert Syst. Appl. 41 (7) (2014) 3333–3342, https://doi.org/10.1016/j.eswa.2013.11.031.

[6] L.V. Kalia, A.E. Lang, Parkinson's disease, Lancet 386 (9996) (2015) 896–912, https://doi.org/10.1016/S0140-6736(14)61393-3.

[7] A.J. Jagadeesan, et al., Current trends in etiology, prognosis and therapeutic aspects of Parkinson's disease: a review, Acta Biomed. 88 (3) (Oct. 2017) 249–262, https://doi.org/10.23750/abm.v88i3.6063.

[8] A. De Rosa, et al., Screening for dopa-responsive dystonia in patients with scans without evidence of dopaminergic deficiency (SWEDD), J. Neurol. 261 (11) (2014) 2204–2208, https://doi.org/10.1007/s00415-014-7477-6.

[9] Ü.Ö. Akdemır, A. Bora Tokçaer, L.Ö. Atay, "Dopamine transporter SPECT imaging in Parkinson's disease and parkinsonian disorders", Turkish, J Med. Sci. 51 (2) (2021) 400–410, https://doi.org/10.3906/sag-2008-253.

[10] H.W. Loh, et al., "Gaborpdnet: Gabor transformation and deep neural network for parkinson's disease detection using eeg signals", Electron. 10 (14) (2021) https://doi.org/10.3390/electronics10141740.

[11] L. Wang, Q. Zhang, H. Li, H. Zhang, SPECT molecular imaging in Parkinson's disease, J. Biomed. Biotechnol. 2012 (2012), https://doi.org/10.1155/2012/412486.

[12] T. Shigekiyo, S. Arawaka, "Laterality of specific binding ratios on DAT-SPECT for differential diagnosis of degenerative parkinsonian syndromes", Sci. Rep. 10 (1) (2020) https://doi.org/10.1038/s41598-020-72321-y.

[13] T.M. Marques, et al., "Identification of cerebrospinal fluid biomarkers for parkinsonism using a proteomics approach", npj Park Dis. 7 (1) (2021) 1–11, https://doi.org/10.1038/s41531-021-00249-9.

[14] S. Shamshirband, M. Fathi, A. Dehzangi, A.T. Chronopoulos, H. Alinejad-Rokny, A review on deep learning approaches in healthcare systems: taxonomies, challenges, and open issues, J. Biomed Inform. 113 (November 2021) (2020) 103627, https://doi.org/10.1016/j.jbi.2020.103627.

[15] T.J. Hirschauer, H. Adeli, J.A. Buford, "Computer-aided diagnosis of Parkinson's disease using enhanced probabilistic neural network", J. Med. Syst. 39 (11) (2015) https://doi.org/10.1007/s10916-015-0353-9.

[16] M. Kim, H. Park, Using tractography to distinguish SWEDD from Parkinson's disease patients based on connectivity, Parkinsons. Dis. 2016 (2016), https://doi.org/10.1155/2016/8704910.

[17] D.Y. Kwon, Y. Kwon, J.W. Kim, Quantitative analysis of finger and forearm movements in patients with off state early stage Parkinson's disease and scans without evidence of dopaminergic deficit (SWEDD), Park. Relat. Disord. 57 (August 2018) (2017) 33–38, https://doi.org/10.1016/j.parkreldis.2018.07.012.

[18] Z. Yu, Y. Li, Association of autonomic symptoms with cerebrospinal fluid biomarkers in Parkinson disease and scans without evidence of dopaminergic deficit, Medicine (baltimore) 100 (7) (2021) e24837.

[19] H. Khachnaoui, N. Khlifa, R. Mabrouk, "Machine learning for early parkinson's disease identification within SWEDD group using clinical and DaTSCAN SPECT imaging features", J. Imaging 8 (4) (2022) https://doi.org/10.3390/jimaging8040097.

[20] R. Mabrouk, B. Chikhaoui, L. Bentabet, Clinical and DaTSCAN SPECT imaging features : a study on parkinson ' s disease and SWEDD, IEEE Trans. Radiat. Plasma Med. Sci. 3 (2) (2019) 170–177.

[21] D.-Y. Kwon, Y.-R. Kwon, J. Ko, J.-W. Kim, Comparison of resting tremor at the upper limb joints between patients with Parkinson's disease and scans without evidence of dopaminergic deficit, Technol. Heal. Care 31 (2023) 515–523, https://doi.org/10.3233/THC-236045.

[22] A. Sarica, A. Quattrone, A. Quattrone, Explainable machine learning with pairwise interactions for the classification of Parkinson's disease and SWEDD from clinical and imaging features, Brain Imaging Behav. (2022), https://doi.org/10.1007/s11682-022-00688-9.

[23] N. Aggarwal, B.S. Saini, S. Gupta, Role of Artificial Intelligence Techniques and Neuroimaging Modalities in Detection of Parkinson's Disease: A Systematic Review, Cogn Comput (2023), https://doi.org/10.1007/s12559-023-10175-.

[24] R. Yamashita, M. Nishio, R.K.G. Do, K. Togashi, Convolutional neural networks: an overview and application in radiology, Insights Imaging 9 (4) (2018) 611–629, https://doi.org/10.1007/s13244-018-0639-9.

[25] H.C. Shin, et al., Deep convolutional neural networks for computer-aided detection: CNN architectures, dataset characteristics and transfer learning, IEEE Trans. Med. Imaging 35 (5) (2016) 1285–1298, https://doi.org/10.1109/TMI.2016.2528162.

[26] F. Segovia, I.A. Illán, J.M. Górriz, J. Ramírez, A. Rominger, J. Levin, Distinguishing Parkinson's disease from atypical parkinsonian syndromes using PET data and a computer system based on support vector machines and Bayesian networks, Front. Comput. Neurosci. 9 (November) (2015) 1–8, https://doi.org/10.3389/fncom.2015.00137.

[27] F. Segovia, et al., "Analysis of 18F-DMFP PET data using multikernel classification in order to assist the diagnosis of Parkinsonism", 2015 IEEE Nucl, Sci. Symp. Med. Imaging Conf. NSS/MIC 2015 (2016) 1–4, https://doi.org/10.1109/NSSMIC.2015.7582227.

[28] T. Shiiba, Y. Arimura, M. Nagano, T. Takahashi, A. Takaki, Improvement of classification performance of Parkinson's disease using shape features for machine learning on dopamine transporter single photon emission computed tomography, PLoS One 15 (1) (2020) 1–12, https://doi.org/10.1371/journal.pone.0228289.

[29] R. Prashanth, S. Dutta Roy, P.K. Mandal, S. Ghosh, High-accuracy classification of parkinson's disease through shape analysis and surface fitting in 123I-ioflupane SPECT imaging, IEEE J. Biomed. Heal. Informatics 21 (3) (2017) 794–802, https://doi.org/10.1109/JBHI.2016.2547901.

[30] K. N. R. Challa V. S. Pagolu G. Panda B. Majhi "An improved approach for prediction of Parkinson's disease using machine learning techniques" *Int. Conf. Signal Process. Commun. Power Embed. Syst. SCOPES 2016 - Proc.* pp. 1446–1451 2017 doi: 10.1109/SCOPES.2016.7955679.

[31] D. Castillo-Barnes, F. J. Martinez-Murcia, A. Ortiz, D. Salas-Gonzalez, J. Ramírez, J. M. Górriz, "Morphological Characterization of Functional Brain Imaging by

Isosurface Analysis in Parkinson's Disease," *Int. J. Neural Syst.*, vol. 30, no. 9, 2020, doi: 10.1142/S0129065720500446.
[32] G. Solana-Lavalle, R. Rosas-Romero, Classification of PPMI MRI scans with voxel-based morphometry and machine learning to assist in the diagnosis of Parkinson's disease, Comput. Methods Programs Biomed. 198 (2021) 105793, https://doi.org/10.1016/j.cmpb.2020.105793.
[33] S. Y. Hsu *et al.* "Feasible classified models for parkinson disease from99mTc-TRODAT-1 SPECT imaging" *Sensors (Switzerland)* vol. 19 no. 7 2019 doi: 10.3390/s19071740.
[34] M. Nithya V. Lalitha K. Paveethra S. Kumari "Early Detection of Parkinson's Disease using Machine Learning Image Processing" *2022 Int. Conf. Comput. Commun. Informatics ICCCI 2022* pp. 25–28 2022 doi: 10.1109/ICCCI54379.2022.9740961.
[35] Z.Y. Shu, et al., Predicting the progression of Parkinson's disease using conventional MRI and machine learning: an application of radiomic biomarkers in whole-brain white matter, Magn. Reson. Med. 85 (3) (2021) 1611–1624, https://doi.org/10.1002/mrm.28522.
[36] R. Mabrouk B. Chikhaoui L. Bentabet "Machine Learning Based Approaches for SWEDD diagnosis in DaTSCAN SPECT imaging" *2017 IEEE Nucl. Sci. Symp. Med. Imaging Conf. NSS/MIC 2017 - Conf. Proc.* no. October 2018 doi: 10.1109/NSSMIC.2017.8532907.
[37] F. Segovia, J.M. Gorriz, J. Ramlrez, D. Salas-Gonzalez, "Multiclass classification of 18F-DMFP-PET data to assist the diagnosis of parkinsonism", PRNI 2016–6th Int, Work. Pattern Recognit. Neuroimaging (2016) 18–21, https://doi.org/10.1109/PRNI.2016.7552342.
[38] M. Rumman A. N. Tasneem S. Farzana M. I. Pavel M. A. Alam "Early detection of Parkinson's disease using image processing and artificial neural network" *2018 Jt. 7th Int. Conf. Informatics Electron. Vis. 2nd Int. Conf. Imaging Vis. Pattern Recognition ICIEV-IVPR 2018* no. February pp. 256–261 2019 doi: 10.1109/ICIEV.2018.8641081.
[39] J. Tang, et al., Artificial neural network-based prediction of outcome in parkinson's disease patients using DaTscan SPECT imaging features, Mol. Imaging Biol. 21 (6) (2019) 1165–1173, https://doi.org/10.1007/s11307-019-01334-5.
[40] S. Chakraborty, S. Aich, H.-C. Kim, 3D textural, morphological and statistical analysis of voxel of interests in 3T MRI scans for the detection of parkinson's disease using artificial neural networks, Healthcare 8 (1) (2020) 34, https://doi.org/10.3390/healthcare8010034.
[41] R. Dehghan M. Naderan S. E. Alavi "Detection of Parkinso's disease using Convolutional Neural Networks and Data Augmentation with SPECT images" *2022 12th Int. Conf. Comput. Knowl. Eng. ICCKE 2022* no. Iccke pp. 1–6 2022 doi: 10.1109/ICCKE57176.2022.9960085.
[42] M. P. Adams B. Yang A. Rahmim J. Tang "Prediction of outcome in Parkinson's disease patients from DAT SPECT images using a convolutional neural network" *2018 IEEE Nucl. Sci. Symp. Med. Imaging Conf. NSS/MIC 2018 - Proc.* no. Iii pp. 4–7 2018 doi: 10.1109/NSSMIC.2018.8824369.
[43] S. Kiryu, et al., Deep learning to differentiate parkinsonian disorders separately using single midsagittal MR imaging: a proof of concept study, Eur. Radiol. 29 (12) (2019) 6891–6899, https://doi.org/10.1007/s00330-019-06327-0.
[44] I. El Maachi, G.A. Bilodeau, W. Bouachir, Deep 1D-Convnet for accurate Parkinson disease detection and severity prediction from gait, Expert Syst. Appl. 143 (2020) 1–27, https://doi.org/10.1016/j.eswa.2019.113075.
[45] T. S. Mian "An Unsupervised Neural Network Feature Selection and 1D Convolution Neural Network Classification for Screening of Parkinsonism" *Diagnostics* vol. 12 no. 8 2022 doi: 10.3390/diagnostics12081796.
[46] A. Tripathi S. K. Kopparapu "CNN based Parkinson's disease assessment using empirical mode decomposition" *CEUR Workshop Proc.* vol. 2699 2020.
[47] M. Nour, U. Senturk, K. Polat, Diagnosis and classification of Parkinson ' s disease using ensemble learning and 1D-PDCovNN, Comput. Biol. Med. 161 (May) (2023) 107031, https://doi.org/10.1016/j.compbiomed.2023.107031.
[48] S. Kaur, H. Aggarwal, R. Rani, Diagnosis of Parkinson's disease using deep CNN with transfer learning and data augmentation, Multimed. Tools Appl. 80 (7) (2021) 10113–10139, https://doi.org/10.1007/s11042-020-10114-1.
[49] T. Verdonck B. Baesens M. Óskarsdóttir and S. vanden Broucke "Special issue on feature engineering editorial" *Mach. Learn.* no. 0123456789 2021 doi: 10.1007/s10994-021-06042-2.
[50] R. Prashanth, S. Dutta, P.K. Mandal, S. Ghosh, International journal of medical informatics high-accuracy detection of early parkinson ' s disease through multimodal features and machine learning, Int. J. Med. Inform. 90 (2016) 13–21, https://doi.org/10.1016/j.ijmedinf.2016.03.001.
[51] S. Hall, Y. Surova, A. Öhrfelt, H. Zetterberg, D. Lindqvist, O. Hansson, CSF biomarkers and clinical progression of Parkinson disease, Neurology 84 (1) (2015) 57–63, https://doi.org/10.1212/WNL.0000000000001098.
[52] A. Arora N. Shoeibi V. Sati A. González-Briones P. Chamoso and E. Corchado "Data augmentation using gaussian mixture model on csv files" *Adv. Intell. Syst. Comput.* vol. 1237 AISC no. June pp. 258–265 2021 doi: 10.1007/978-3-030-53036-5_28.
[53] C. Shorten, T.M. Khoshgoftaar, A survey on image data augmentation for deep learning, J. Big Data 6 (1) (2019) 60, https://doi.org/10.1186/s40537-019-0197-0.
[54] G. Pahuja, B. Prasad, Deep learning architectures for Parkinson ' s disease detection by using multi-modal features, Comput. Biol. Med. 146 (January) (2022) 105610, https://doi.org/10.1016/j.compbiomed.2022.105610.
[55] H. Choi, S. Ha, H.J. Im, S.H. Paek, D.S. Lee, Refining diagnosis of Parkinson's disease with deep learning-based interpretation of dopamine transporter imaging, Neuroimage Clin. 16 (September) (2017) 586–594, https://doi.org/10.1016/j.nicl.2017.09.010.
[56] F.J. Martinez-Murcia, et al., "A 3D convolutional neural network approach for the diagnosis of parkinson's disease BT -, Natural and Artificial Computation for Biomedicine and Neuroscience" (2017) 324–333.
[57] M. Hires, M. Gazda, L. Vavrek, P. Drotar, "Voice-specific augmentations for parkinson's disease detection using deep convolutional neural network", SAMI 2022 - IEEE 20th Jubil. World Symp. Appl. Mach. Intell. Informatics Proc. (2022) 213–218, https://doi.org/10.1109/SAMI54271.2022.9780856.
[58] T.T. Um, et al., "Data augmentation of wearable sensor data for Parkinson's disease monitoring using convolutional neural networks", ICMI 2017 - Proc. 19th ACM Int. Conf. Multimodal Interact. 2017-Janua (2017) 216–220, https://doi.org/10.1145/3136755.3136817.
[59] E. Dzotsenidze, E. Valla, S. Nõmm, K. Medijainen, P. Taba, A. Toomela, Generative adversarial networks as a data augmentation tool for CNN-based parkinson's disease diagnostics, IFAC-PapersOnLine 55 (29) (2022) 108–113, https://doi.org/10.1016/j.ifacol.2022.10.240.
[60] M. Alissa, et al., Parkinson's disease diagnosis using convolutional neural networks and figure-copying tasks, Neural Comput. Appl. 34 (2) (2022) 1433–1453, https://doi.org/10.1007/s00521-021-06469-7.
[61] X. Yang, Q. Ye, G. Cai, Y. Wang, G. Cai, "PD-ResNet for classification of parkinson's disease from gait", IEEE J. Transl. Eng. Heal. Med. 10 (May) (2022) https://doi.org/10.1109/JTEHM.2022.3180933.